Which spectral lines trace what physical processes in the Galactic Center? First results: line identification

Alyssa Bulatek (she/her)[1], Adam Ginsburg[1], Katharina Immer[2], Desmond Jeff[1]

1. University of Florida, 2. University of Leiden

Motivation

In the disk of the Milky Way, certain molecules are used as "rule of thumb" tracers for processes in the interstellar medium. Some example processes/tracers include:

- *Outflows from protostars:* high-velocity isotopologues of CO (carbon monoxide)
- *Hot star-forming cores:* CH_3OH (methanol), CH_3CN (methyl cyanide)
- *Low-velocity shocks:* SiO (silicon monoxide), HNCO (isocyanic acid)
- *Dense gas:* HCN (hydrogen cyanide), HCO+ (formyl cation)

In extreme environments like the centers of galaxies, these tracers fail. CO is self-absorbed in the Galactic Center. SiO is sparse in locations with less star formation than Sgr B2. The Central Molecular Zone (CMZ) is very dense (10^4 to 10^7 cm^{-3}) (Morris and Serabyn 1996), so traditional dense gas tracers are bright everywhere. The same is true for tracers of hot cores and shocks. **We need unique tracers for star formation processes that can be used in CMZs and starburst galaxies.**

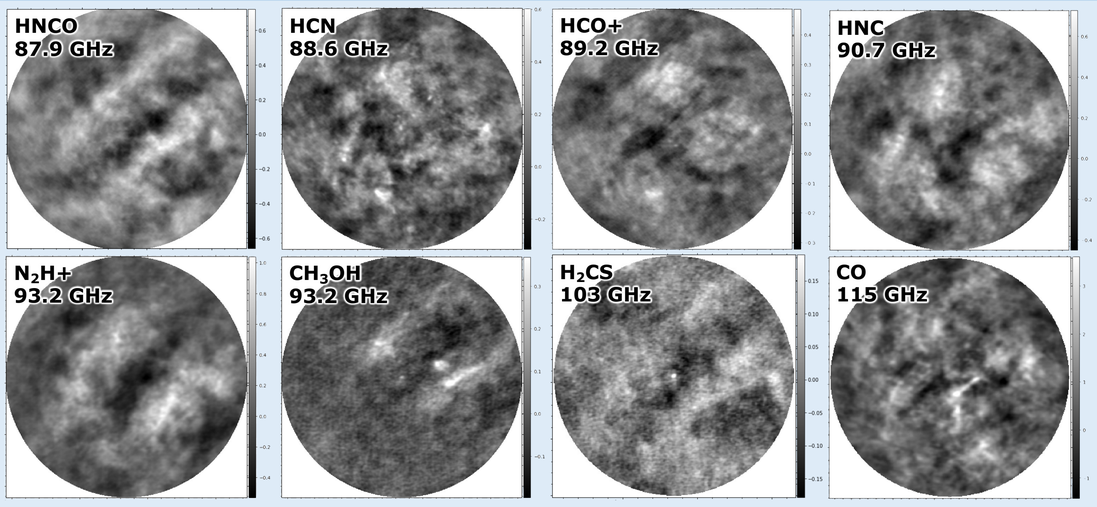

Figure 1. Integrated intensity maps (in units of Jy beam^{-1} km s^{-1}) of molecules near the water maser in The Brick. Though there are a few molecules that have some coherence, many molecules reveal the complicated underlying structure of the CMZ: multiple layers of turbulent material.

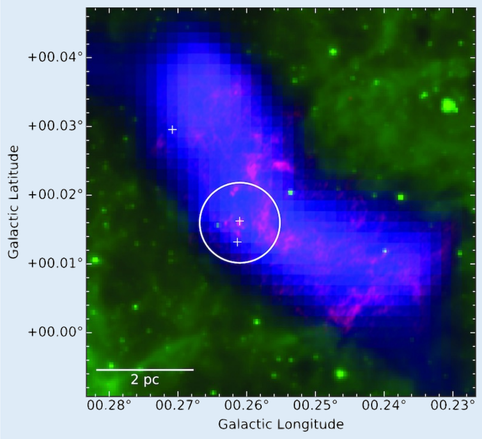

G0.253+0.016, a.k.a. "The Brick"

- One of the densest CMZ clouds (> 10^4 cm^{-3})
- No widespread signs of SF, except:
- Water masers (white crosses), one of which is coincident w/ continuum source
  - Maser core is driving an outflow (traced by high-velocity SiO) and is surrounded by both turbulent/shocked and quiescent gas

Figure 2. Three-color image of The Brick adapted from Walker et al. (2021). Red: ALMA 3 mm dust continuum (Rathborne et al. 2014); green: *Spitzer*/GLIMPSE 8 μm emission (Churchwell et al. 2009), blue: *Herschel*/HiGAL dust column density (Battersby et al. 2011; Molinari et al. 2016).

The Survey

Telescope	Atacama Large Millimeter/submillimeter Array (ALMA) 12-m
Pointing	"maser core" in The Brick, same as Walker et al. (2021)
Frequency coverage	Bands 3, 4, and part of 6 (Bands 5 through 7 pending)
Angular resolution	1.72" by 1.40" (about 0.07 pc)

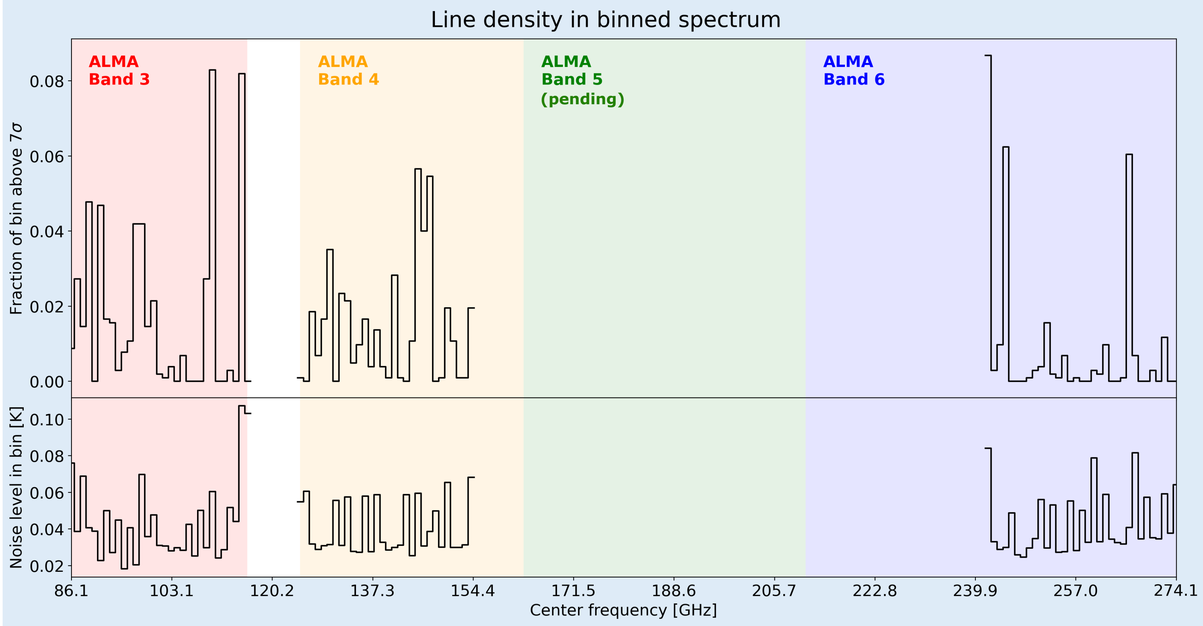

Figure 3. Density of spectral lines in a 1 GHz-binned representation of the delivered survey data so far. This density was calculated from peak intensity spectra, which trace localized emission (in many frames, this is the central maser source). The field-of-view across all spectral windows was limited to 0.8 times the primary beam size of the highest-frequency spectral window in our data, at the top of Band 6.

Temperature and Column Density in the Hot Core

Temperature-sensitive molecules, **e.g., CH_3CN (methyl cyanide)**: "ladder" of *k*-components, heights are related to physical environment

→ Extract spectra from brightest pixel, use **XCLASS** to model synthetic CH_3CN spectra at given temperature and column density

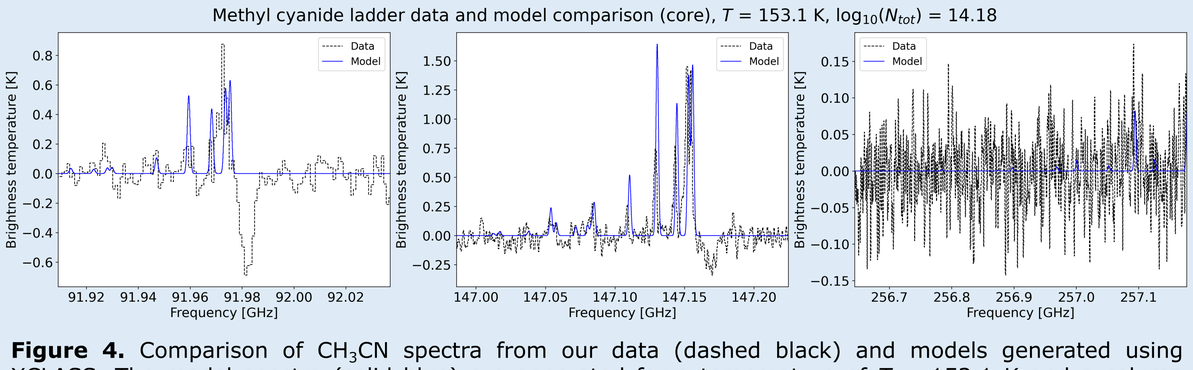

Figure 4. Comparison of CH_3CN spectra from our data (dashed black) and models generated using XCLASS. The model spectra (solid blue) are generated for a temperature of T = 153.1 K and a column density of $\log_{10}(N_{tot})$ = 14.18.

Morphologies

outflow cavity | outflow + core | core

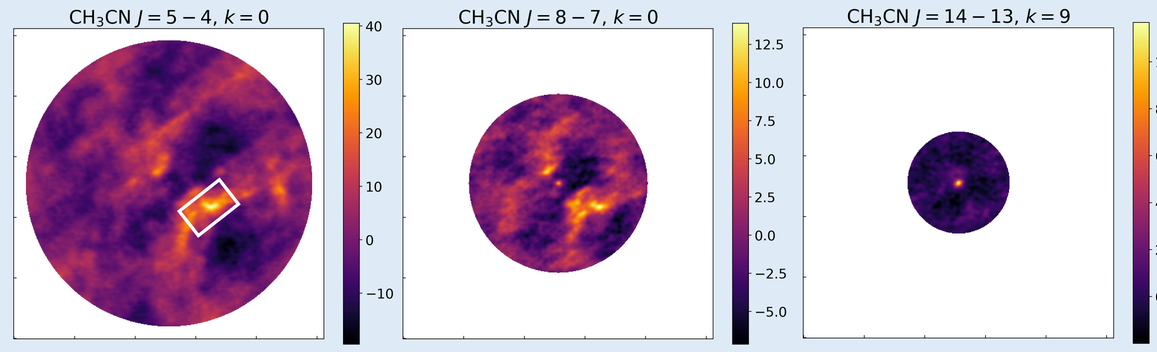

Figure 5. Integrated intensity maps (in units of K km s^{-1}) of CH_3CN. Each map isolates one *k*-component in each ladder. Both the J = 5 and J = 8 ladders show the diffuse gas surrounding the outflow cavity, but the J = 5 ladder does not recover the central hot core. The J = 8 and J = 14 ladders both recover the hot core, but the J = 14 ladder does not show the diffuse outflow cavity. The J = 5 ladder shows the cutout where we extracted a mean spectrum from the outflow cavity edge (white rectangle).

Molecules in the Hot Core

Temperature/column density estimates from fitting CH_3CN ladders → Assuming the same values for all molecules, produce **full LTE model**

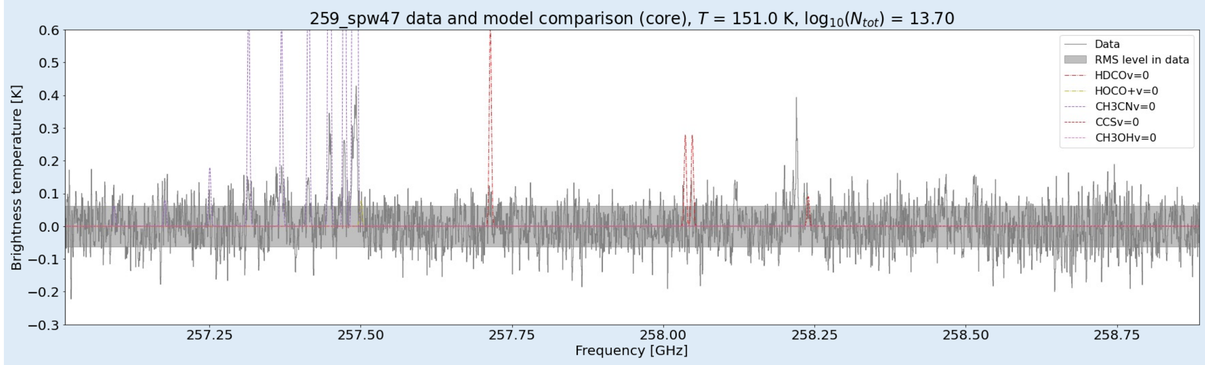

Figure 6. Comparison of data (solid grey) and model (non-solid, colorful) spectra generated with XCLASS in the maser core. Each molecule is modeled separately with XCLASS. The CH_3CN J = 14 ladder shows up in the spectrum for the maser core. The temperature and column density used to generate the models are very close to the estimates we gleaned from our initial CH_3CN fitting, but these values likely do not apply to all transitions of all molecules. This is why the strength of the model lines does not match the data.

Molecules in the Outflow Cavity

Generate the same spectra, but now for the outflow cavity edge (see Fig. 5)

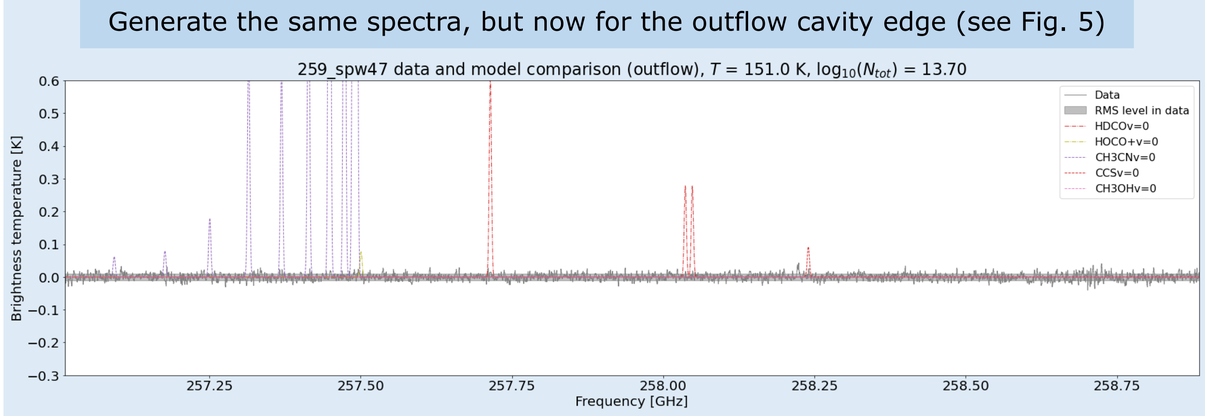

Figure 7. Comparison of data (solid grey) and model (non-solid, colorful) spectra generated with XCLASS in the outflow cavity edge. Each molecule is modeled separately. The CH_3CN J = 14 ladder does not show up in the spectrum for the outflow. The temperature and column density used to generate the models are very close to the estimates we gleaned from our initial CH_3CN fitting, but these values likely do not apply to all transitions of all molecules. This is why the strength of the model lines do not match the data.

Table 1. A preliminary, non-exhaustive list of molecules detected in our pointing.

2 atoms	3 atoms	4 atoms	5 atoms	6 atoms	7 atoms	8 atoms	9 atoms	10 atoms
CO	OCS	H_2CS	C_4H	CH_3CN	CH_3CHO	CH_3OCHO	CH_3OCH_3	$(CH_3)_2CO$
$C^{17}O$	CCH	HNCO	HC_3N	CH_3OH	CH_3CCH		$CH_3{}^{13}CH_2CN$	
CS	CCS	HDCO	$H^{13}CCCN$	CH_3OD	CH_2CHCN		$CH_3CH_2{}^{13}CN$	
^{13}CS	HCN	HOCO+	$HC^{13}CCN$	CH_2DOH			g-CH_3CH_2OH	
CN	$H^{13}CN$	SO_3	$HCC^{13}CN$	$^{13}CH_3OH$				
^{13}CN	$HC^{15}N$		CH_2NH	NH_2CHO				
SiO	HNC		c-HCCCH					
NO	$HN^{13}C$							
NS	NaCN							
AlF	NaNC							
$Al^{37}Cl$	SO_2							
NaCl	$^{34}SO_2$							
SO+	$Si^{13}CC$							
	SiC_2							
	$^{30}SiC_2$							
	HCO+							
	$H^{13}CO+$							
	N_2H+							

References

Arce et al. 2010, ApJ, 715, 1170.
Battersby et al. 2011, A&A, 535, A128.
Churchwell et al. 2009, PASP, 121, 213.
Ginsburg et al. 2016, A&A, 586, A50.
Kauffmann et al. 2017, A&A, 603, A89.
Lu et al. 2021, ApJ, 909, 177.
Molinari et al. 2016, A&A, 591, A149.
Morris et al. 1996, ARA&A, 34, 645.
Rathborne et al. 2014, ApJ, 786, 140.
Walker et al. 2021, MNRAS, 503, 77.

Email: abulatek@ufl.edu **Website:** abulatek.github.io